Title

A T1 and DTI fused 3D corpus callosum analysis in MCI subjects with high and low cardiovascular risk profile

Permalink

https://escholarship.org/uc/item/93z4v5r4

Authors

Lao, Yi
Nguyen, Binh
Tsao, Sinchai
et al.

Publication Date

2017

DOI

10.1016/j.nicl.2016.12.027

Copyright Information

Peer reviewed
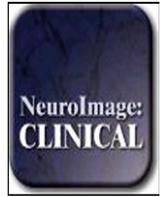
A T1 and DTI fused 3D corpus callosum analysis in MCI subjects with high and low cardiovascular risk profile

Yi Lao[a,b,1], Binh Nguyen[a], Sinchai Tsao[a], Niharika Gajawelli[a,b], Meng Law[b,d], Helena Chui[b,d], Michael Weiner[e], Yalin Wang[c], Natasha Leporé[*,a,b,1]

[a]CIBORG Laboratory, Department of Radiology, Children's Hospital Los Angeles, USA
[b]Department of Biomedical Engineering, University of Southern California, USA
[c]School of Computing, Informatics, and Decision Systems Engineering, Arizona State University, USA
[d]Department of Radiology, Keck School of Medicine, University of Southern California, USA
[e]Department of Radiology, University of California, San Francisco, USA

ABSTRACT

Understanding the extent to which vascular disease and its risk factors are associated with prodromal dementia, notably Alzheimer's disease (AD), may enhance predictive accuracy as well as guide early interventions. One promising avenue to determine this relationship consists of looking for reliable and sensitive *in-vivo* imaging methods capable of characterizing the subtle brain alterations before the clinical manifestations. However, little is known from the imaging perspective about how risk factors such as vascular disease influence AD progression. Here, for the first time, we apply an innovative T1 and DTI fusion analysis of 3D corpus callosum (CC) on mild cognitive impairment (MCI) populations with different levels of vascular profile, aiming to de-couple the vascular factor in the prodromal AD stage. Our new fusion method successfully increases the detection power for differentiating MCI subjects with high from low vascular risk profiles, as well as from healthy controls. MCI subjects with high and low vascular risk profiles showed differed alteration patterns in the anterior CC, which may help to elucidate the inter-wired relationship between MCI and vascular risk factors.

© 2017 The Authors. Published by Elsevier Inc. This is an open access article under the CC BY-NC-ND license (http://creativecommons.org/licenses/by-nc-nd/4.0/).

1. Introduction

Emerging evidence has shown that cardiovascular disease (CVD) and preclinical cardiovascular risk factors are linked to the etiology of dementia, including Alzheimer disease (AD) (Cardenas et al., 2012; Gorelick et al., 2011; Iadecola, 2013; Kalaria et al., 2012; Luchsinger et al., 2001; Newman et al., 2005; Posner et al., 2000; Vermeer et al., 2003). Specifically, some findings suggest a direct influence of vascular diseases in accelerating amyloid β accumulation (Garcia-Alloza et al., 2011; Iadecola, 2013). The entanglement of cardiovascular and neural factors is further evidenced by the recently hypothesized connection between the Locus Coeruleus (LC) and AD. In this scenario, AD is mediated by the integrated modulatory function of LC on

the heart rate, attention memory, and cognitive functions (Mather and Harley, 2016). While an effective treatment for AD is still out of reach, there are established therapeutic strategies for CVD, and its risk factors are also clinically modifiable (Chui, 2006). Therefore, disentangling the effects of CVD and its risk factors on the development of AD has implication for symptom management, and may potentially alter clinical outcomes for pre-dementia patients.

In particular, differentiating the effects of different CVD profiles on the anatomy of the brain in mild cognitive impairment (MCI) - a precursor to AD and other types of dementia - would provide important insights into the effects of preventable CVD factors on the initial course of AD. Nevertheless, efforts aimed at differentiating vascular diseases from MCI report inconsistent results (Hayden et al., 2005; Loewenstein et al., 2006; Nordlund et al., 2007). In particular, Hayden et al. identified a set of memory and executive tests in prodromal vascular dementia (VaD) that are distinguishable from prodromal AD (Hayden et al., 2005). Nordlund et al. confirmed the differences in executive function between MCI subjects with and without vascular disease, and also reported differences in speed, attention, and visuospatial functions in these two groups (Nordlund et al., 2007).

* Corresponding author at: CIBORG Laboratory, Department of RadiologyUniversity of Southern California & Children's Hospital Los Angeles,4650 Sunset Blvd, Los Angeles, CA90027, USA.
  E-mail address: natashalepore@gmail.com (N. Leporé).
[1] Equal senior author contribution.

However, no differences between vascular and non-vascular types of MCI were found by other studies (Loewenstein et al., 2006). These discrepancies may partially be caused by different inclusion criteria for vascular disease (i.e. with or without stroke), coupled to analysis techniques that do not have the required detection sensitivity. This highlights the need for sensitive and reliable algorithms that can help in decoupling the vascular component of preclinical dementia, and thus aid in early diagnosis and therapeutic design.

Being the largest white matter (WM) structure with a high demand of blood supply from several main arterial systems, the corpus callosum (CC) has been reported to be vulnerable to both MCI (Di Paola et al., 2010; Dimitra et al., 2013; Teipel et al., 2011; Zhang et al., 2013) and vascular diseases (Delano-Wood et al., 2010; Friedman et al., 2014; Gons et al., 2012). Given the extensive connections between the CC and the cortex, regional disturbances of the CC may mirror dysfunctions of specific cortical domains. Therefore, anatomical alterations of the CC may serve as potential discriminators of the concurrent but possibly different effects of vascular and neurodegenerative components. Structural magnetic resonance imaging (MRI) is a typical choice for detecting CC anatomical alterations and has been effective in deciphering brain parenchyma loss (Serra et al., 2010; Teipel et al., 2002; Wang et al., 2011a; Zhu et al., 2012), while diffusion tensor imaging (DTI) has been promising in characterizing WM microstructure alterations (Dimitra et al., 2013; Kantarci et al., 2005; Teipel et al., 2011; Zhang et al., 2013). Parenchyma and diffuse injuries often occur concomitantly in WM structures such as the CC, and a joint analysis of diffusion and T1-weighted data may therefore provide a more complete picture of CC changes brought on by brain injury. However, to the best of our knowledge, all the above studies regarded each aspect on its own (Dimitra et al., 2013; Wang et al., 2011a; Zhang et al., 2013), or by comparing them side-by-side (Di Paola et al., 2010; Teipel et al., 2011). None have tried to truly combine these two features into one analysis.

Here, we perform an innovative, truly combined analysis of structural and diffusion MRI data on the 3D CC surfaces of MCI subjects. We group our MCI subjects into high and low vascular risk profiles (will be referred to as MCI-l and MCI-h groups in the remainder of the text), and conduct pairwise statistical analyses on the fused morphological and diffusion properties among these two MCI subgroups as well as on aging controls without cognitive impairment. Our aims are twofold: 1) to test whether the vascular component affects distinct regional alterations that may help us to distinguish different MCI subtypes; 2) to further validate the feasibility and sensitivity of using our T1 and DTI fusion method to analyze subcortical alterations.

2. Subjects and methodologies

2.1. Data and preprocessing

Fifty-eight subjects aged 66 to 89 were grouped based on their clinical dementia rating (CDR) and vascular risk profile into 15 MCI subjects with low vascular risk (76.40±7.65 years, CDR=0.5, low Framingham cardiovascular risk profile (FCRP) scores), 18 MCI subjects with high vascular risk (78.39±5.69 years, CDR = 0.5, high FCRP scores or had previous clinical diagnosis of myocardial infarction) and 25 healthy controls (76.68±6.40 years). Subjects with confounding neurological conditions, such as stroke, were excluded. Brain T1 and DT-MR scans of all the subjects were obtained using a 3T SIEMENS scanner. DTI data were acquired using an echo-planar imaging sequence, with a voxel size of $2 \times 2 \times 2 \ mm^3$, resolution of $128 \times 128 \times 60$, b-value of 1000s/mm², and 60 gradient directions. Anatomical data were acquired using a MPRAGE sequence, with a voxel size of $1 \times 1 \times 1 \ mm^3$, resolution of $256 \times 256 \times 192$, TE=2.98 ms, TR=2500 ms, and TI=1100 ms. Each subject,

in addition to being imaged via T1-MRI and DTI, was evaluated on the MMSE (Mini-Mental State Exam) as a marker of cognitive function, as well as a standardized battery of neuropsychological tests, consisting of MEMSC (verbal memory summary score) for verbal memory, NVMEMSC (non-verbal memory summary score) for non-verbal memory, EXECSC (executive function summary score) to measure executive function, and GLOBSC (global cognition summary score) to assess global cognition. These measures have previously been described in the literature and are commonly used in neuropsychological assessments (Mungas et al., 2003).

All the T1 data were preprocessed and linearly registered to the same template space - selected randomly from one of the controls that was previously transformed to MNI space (Jenkinson et al., 2002). On the linearly registered T1 images, each subject's corpus callosum (CC) was manually traced on the mid-sagittal plane, and the lateral boundaries were determined where the CC starts to radiate into and merge with cerebral white matter. Subsequently, 3D surface representations and conformal mesh grids of the CC were constructed using an in-house conformal mapping program (Wang et al., 2011b). One-to-one correspondence between vertices were obtained through constrained harmonic based registration (Wang et al., 2011b).

All the DTI data were first preprocessed, which included brain masking, eddy current correction, echo-planar imaging distortion correction, and tensor estimation. To truly integrate DTI and T1 information, we transformed the DT images from each subject to their corresponding T1 space, using linear registration between the b0-weighted and T1 images. The linear transformation matrices saved from the T1 registration were then applied on the linearly aligned b0 images, to transform the diffusion information to the space of the T1 template. After each of the linear registrations, the diffusion tensors were resampled using the b0 transformation matrices, and rotated according to the underlying anatomy. These steps were achieved using MedINRIA (Toussaint et al., 2007).

2.2. Surface based sampling

After the surface based registration in Section 2.1, a deformation tensor $\sqrt{JJ^T}$ - where J is the Jacobian of the transformation from the registration - was computed at each vertex on the surface. Its determinant (det$J$, the difference in surface area) and projection on the log-Euclidean space (log $\sqrt{JJ^T}$) (Arsigny et al., 2006) were used in later statistical analysis (Lepore et al., 2008; Wang et al., 2011b).

To project diffusion indices of each of the CCs onto its surface, we first calculated midlines of all the 3D CCs, and then collected diffusion parameters to each surface vertex along its corresponding radius to the midline, specifically using:

$$\left\| \frac{\left(\overrightarrow{X - M} \right) \times \left(\overrightarrow{P - M} \right)}{\left\| \overrightarrow{X - M} \right\|} \right\| \leq R. \tag{1}$$

and

$$\left(\overrightarrow{X - P} \right) \cdot \left(\overrightarrow{P - M} \right) \geq 0. \tag{2}$$

Here X, M, P are the (x, y, z) coordinates of a vertex in the surface, the corresponding point of the vertex in the midline, and a voxel within the 3D representations, respectively, while R represents a pre-defined distance between P to the line of $\overrightarrow{X - M}$. The sampling process can be more intuitively visualized in Fig. 1. The first equation is used to assign the voxels close enough ($\leq R$) to the corresponding radius of the vertex, while the second equation constrains the sampling to the voxels within the space between the midpoint to the vertex (not in the prolongation direction). According to our previous
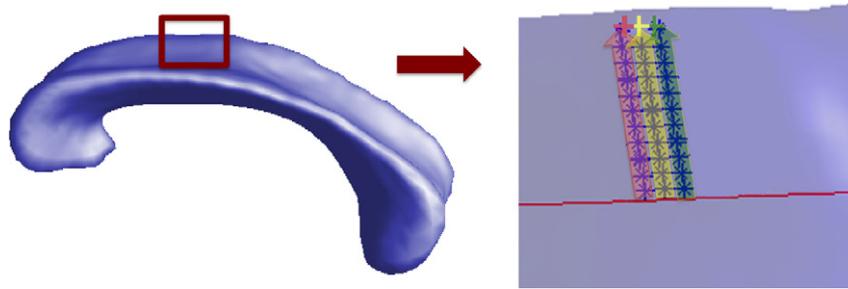
Fig. 1. Surface of CC and the illustration of sampled voxels. The red line on the right side of the figure is the midline of the CC, blue stars represent voxels within CC, and pink, yellow, as well as green crosses represent surface vertices. In the direction perpendicular to the midline and pointing to each vertex, voxels within pink, yellow, and green areas are projected to the vertices with the corresponding colors. Mean index (FA, MD....) of projected voxels is assigned to the vertex for later statistics.

pilot study, we chose $R = 0.6\ mm^3$ to make sure each of the vertices has some voxels assigned, and to minimize overlap with neighboring vertices (Lao et al., 2015).

2.3. Statistical analysis

Our statistical analyses were conducted using either the morphometry information, the diffusion information, or a combination of both. Vertex-wise univariate student t-tests or multivariate Hotelling's T^2 tests were performed based on the following variables:

1. Morphometry information: univariate det$J$ and multivariate $(s1, s2, s3)$ from the logged deformation tensors, which are independent elements of the matrix (Fig. 2, 1st and 2nd row).
2. Diffusion information: univariate mean FA along the radius of the CC for each vertex and multivariate λ_1 and λ_2 (Fig. 2, 3rd and 4th row). Note: we did not include λ_3. Being small, this value is susceptible to noise and may reduce detection power. While this is fine for additive measures such as FA as the effect will be negligible (as the value is small), it is a much bigger issue when analyzing a multivariate vector of statistics, where each eigenvalue is treated as an independent measure.
3. A fusion of morphometry $(s1, s2, s3)$ and diffusion indices $(\lambda_1$ and $\lambda_2)$ (Fig. 2, 5th row).

Here, one of the primary purposes is to determine a method that can sensitively detect underlying anatomical differences between our MCI groups. Therefore, our general criteria for measurements selection were: firstly, to use the most representative, or generally used measurements in both shape and diffusion analysis for comparison, and secondly, to compare these to what we hypothesized would be a joint structural and diffusion measure with enough sensitivity to detect subtle underlying differences between groups, based on ours and others prior studies. MD showed significant but less powerful results than FA, and similarly, $(FA, s1, s2, s3)$, or $(MD, s1, s2, s3)$ showed less significant results than $(\lambda_1, \lambda_2, s1, s2, s3)$. Therefore, we only included the above five most representative univariate or multivariate measurements in our final analysis.

Given the fact that our subjects were from a relatively large age range (66–89 years), we used linear regression to factor out the effect of age. For each feature value separately, we have:

$$F = \beta_0 + \beta_1 * age + \beta_2 * group + error. \qquad (3)$$

Where F is one of the features we previously obtained, β_0, β_1, β_2 are the corresponding correlation coefficients. Group are coded as dummy variable: 0 for controls, 1 for MCI-l group, and 2 for MCI-h group. All the following statistics were performed on linearly regressed features.

For each of the tests, two types of permutations were performed: a vertex-based one to avoid the normal distribution assumption and one over the whole segmented image to correct for multiple comparisons, as described in (Lepore et al., 2008; Nichols and Holmes, 2001). Permutation based corrections are independent of the distributions of the statistics, which is commonly non-parametric in voxel- or vertex-wise analyses. Furthermore, permutation based multiple comparison corrections are less stringent than conventional sequential correction methods (Benjamini and Hochberg, 1995), as they do not assume independence of neighboring voxels or vertices, and they are widely accepted in brain image analyses (Lepore et al., 2008; Rajagopalan et al., 2012; Wang et al., 2009). In each of the permutation tests, 10,000 permutations were employed.

2.4. Correlation analysis

The imaging measurements were further evaluated with respect to overall mental status demonstrated by Mini Mental State Examination scores, as well as 4 domain specific neuropsychological measurements: MEMSC, NVMEMSC, EXECSC, GLOBSC. Four subjects with missing neuropsychological test data were excluded, leaving a total of 54 subjects for the correlation analysis. After controlling for age, Pearson's correlation analyses were conducted to determine specific contributions of regional CC to cognitive performance, in terms of shape (represented by det$J$) or WM integrity (represented by mean FA). To evaluate the association of neuropsychological performances with the combined feature of shape and diffusion properties of CC (represented by $(\lambda_1, \lambda_2, s1, s2, s3)$), we continued to perform a distance correlation – a generalization to the classical bivariate measurements of dependance (Székely et al., 2009). Similar to the permutation corrections employed in group-wise comparisons, 10,000 permutations were applied in each of the correlation tests, as described in Lao et al. (2014), Nichols and Holmes (2001).

3. Results

Fig. 2 shows vertex-wise group differences among 3 groups based on 5 different measures: det$J$, $(s1, s2, s3)$, mean FA, (λ_1, λ_2), and fused $(\lambda_1, \lambda_2, s1, s2, s3)$. The corresponding structure-wise corrected $p-$ values are displayed in Table 1. The final statistical results on the CC surface in Fig. 2 are smoothed using heat kernel algorithm as described in Chung et al. (2005).

The MCI-l group showed alterations spanning the midbody and the posterior surface of the CC as compared to controls, with significant structure-wise differences detected by det$J$, $(s1, s2, s3)$, and $(\lambda_1, \lambda_2, s1, s2, s3)$ measurements; the MCI-h group presented broad areas of alterations mainly located in the dorsal anterior, mid-body, and splenium of the CC compared to controls, with significant structure-wise differences detected by det$J$, $(s1, s2, s3)$, and $(\lambda_1, \lambda_2, s1, s2, s3)$ measurements, as well as trends detected by
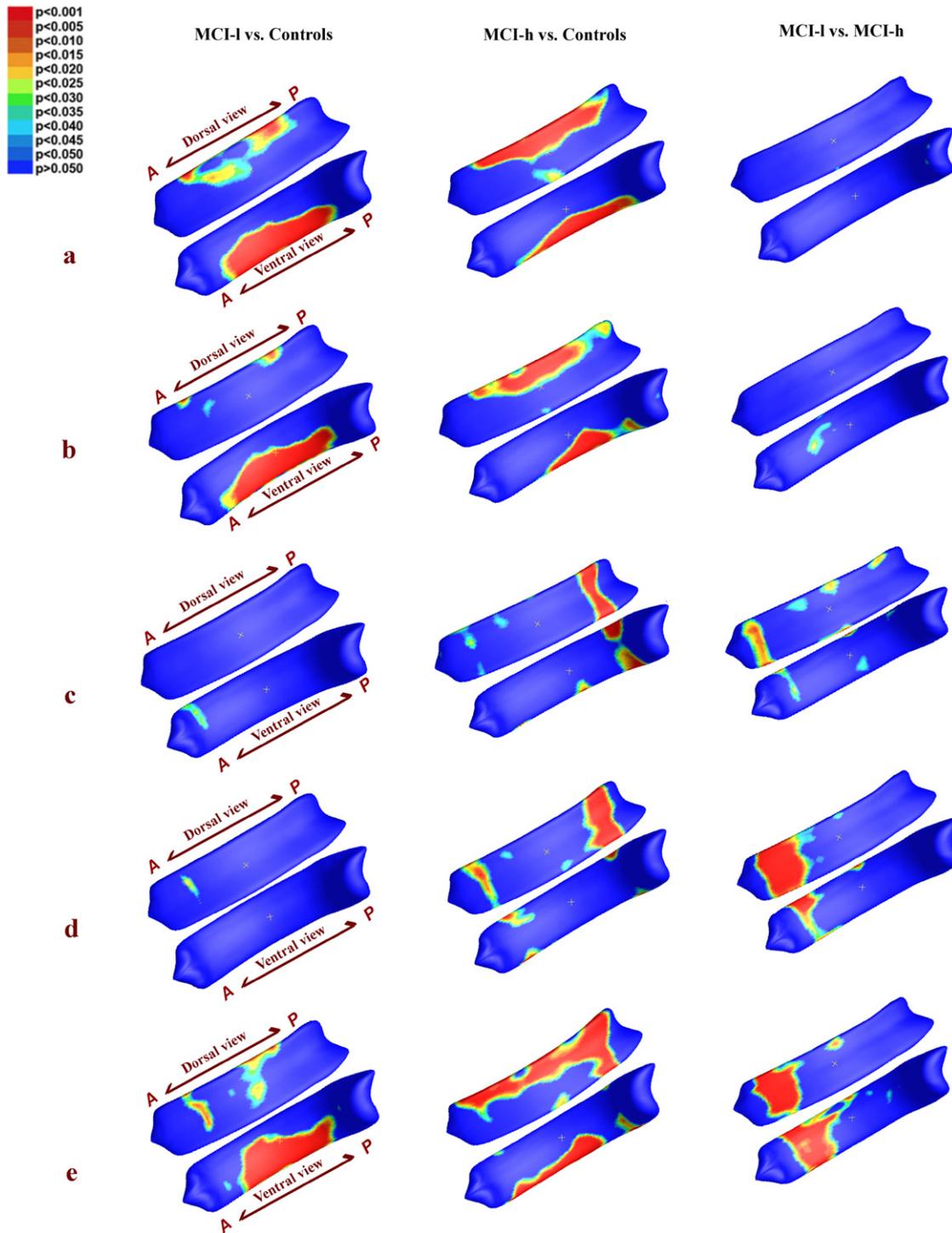
Fig. 2. Group analysis of MCI-l vs. controls (1st column), MCI-h vs. controls (2nd column), and MCI-l vs. MCI-h (3rd column) using 5 different measures: a) det$J$; b) ($s1, s2, s3$); c) mean FA; d) (λ_1, λ_2); e) ($\lambda_1, \lambda_2, s1, s2, s3$). Vertex-wise corresponding p−values are color-coded according to the color bar in the upper left corner. P- maps are smoothed using heat kernel algorithm (Chung et al., 2005). In addition, whole structure-wise corrected p−values are presented in Table 1.

mean FA and (λ_1, λ_2) measurements. For the MCI-h vs. MCI-l, the main clusters were located in the genu of the CC, and the fusion measurements reached structure-wise significance, while mean FA and (λ_1, λ_2) showed trends. It is important to note that up-sampling the relatively low resolution DTI data resulted in same or similar diffusion indices appearing in surrounding vertices on the CC surface, thus causing the band-like areas shown in the significance map (Fig. 2).

To intuitively understand the direction of alterations, we also mapped the average maps of vertex-wise det$J$ and FA between 3 groups, as shown in Fig. 3. Compared Fig. 3 with Fig. 2, we can see that nearly all the significance areas fell in the Controls > MCI-l, Controls > MCI-h, as well MCI-l > MCI-h areas. These findings point to shrinkage and reduced WM integrity in the CCs of MCI-l and MCI-h patients as compared to those of normal controls.

Table 1

Structure-wise corrected $p-$values for different measurements are displayed. All the p-values were corrected using a permutation based analysis with 10,000 permutations. Significance is set to $p < 0.05$, and is highlighted in light cyan. P-values implying trends are highlighted in light gray.

Measurements	MCI-l vs. ctls	MCI-h vs. ctls	MCI-l vs. MCI-h
$\det J$	0.0309	0.0292	0.9901
$(s1, s2, s3)$	0.0425	0.0415	0.1550
FA	0.4810	0.0815	0.0813
(λ_1, λ_2)	0.3440	0.0731	0.0673
$(\lambda_1, \lambda_2, s1, s2, s3)$	0.0173	0.0153	0.0107

Table 2

Structure-wise corrected $p-$values for different measurements are displayed. All the p-values were corrected using a permutation based analysis with 10,000 permutations. Significance is set to $p < 0.05$, and is highlighted in light cyan. P-values implying trends are highlighted in light gray.

Measurements	$\det J$	mean FA	$(\lambda_1, \lambda_2, s1, s2, s3)$
MMSE	0.5290	0.1639	**0.7184**
MEMSC	0.3322	0.0147	**0.2886**
NVMEMSC	0.2902	0.2736	**0.3857**
EXECSC	0.0411	0.0857	**0.0066**
GLOBSC	0.0131	0.0208	**0.0048**

3.1. Correlation analysis results

The vertex-wise significant $p-$map and correlation coefficients r map from Pearson's correlation analyses between neuroanatomical measurements ($\det J$ and mean FA) and 5 neuro-cognitive indices

(MMSE, MEMSC, NVMEMSC, EXECSC, GLOBSC) are displayed in Fig. 4 and Fig. 5. The corresponding structural-wise corrected $p-$ values are shown in Table 2.

For surface shape measurements, represented by $\det J$, significant regional correlations are seen in clusters mainly located in anterior and posterior CC, and two of the five correlation tests (EXECSC and GLOBSC) hit structure-wise significances according to Table 2. As to WM integrity, represented by mean FA along radial direction, four of the five correlation tests (MMSE, MEMSC, EXECSC, and GLOBSC) showed anatomical meaningful correlations with WM integrity in the dorsal anterior CC. According to Table 2, EXECSC showed a structure-wise correlation with mean FA that represented a trend ($p = 0.0857$), and 2 of the 5 measurements (MEMSC and GLOBSC) reached structure-wise significance. As to the combined shape and diffusion features ($\lambda_1, \lambda_2, s1, s2, s3$), areas of significant correlations are mainly consistent with those detected by shape and WM integrity separately, while nonverbal memory scores (NVMEMSC) showed anatomical meaningful correlations in the posterior CC, which were not fully captured by shape or diffusion feature based bivariate correlations.

4. Discussion and conclusion

In our study, the MCI-h group presented widespread atrophy and reduced WM integrity spanning nearly the whole CC as compared to controls, with the largest cluster located on the posterior end. In the group analysis between the MCI-l group and the controls, similar alterations were mainly shown in the middle to the posterior regions. When comparing the MCI-h and the MCI-l group, our fusion method detected significant disparities in the dorsal anterior CC. These findings together indicate a consistent influence of MCI on the midbody to the posterior end of the CC, and importantly, a distinct effect of cardiovascular profile on the genu. Moreover, these same regions presented significant correlations with neurophysiological battery tests including MEMSC, EXECSC, and GLOBSC. Our findings provide important anatomical supports to the co-existence of MCI-subtypes and may yield new insights in the distinct role of cardiovascular components in the etiology of dementia. The T1 and
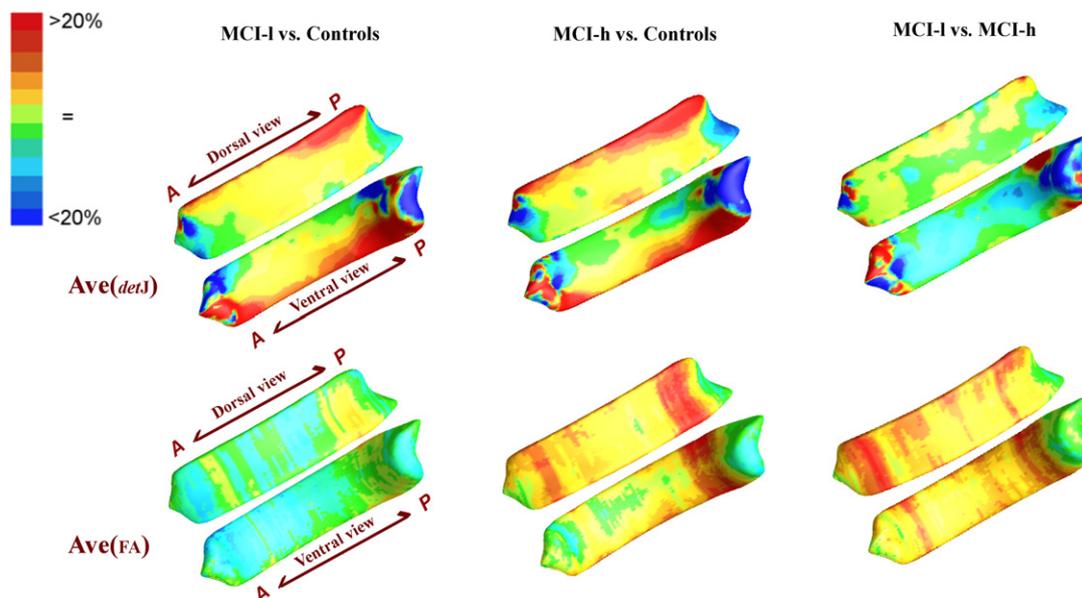

Fig. 3. Average map of $\det J$ and mean FA between groups are color-coded according to the color bar in the upper left corner. When these results are compared with Fig. 2, we can see the main direction of change: nearly all the significance areas fell in the Controls > MCI-l, Controls > MCI-h, as well MCI-l > MCI-h areas.
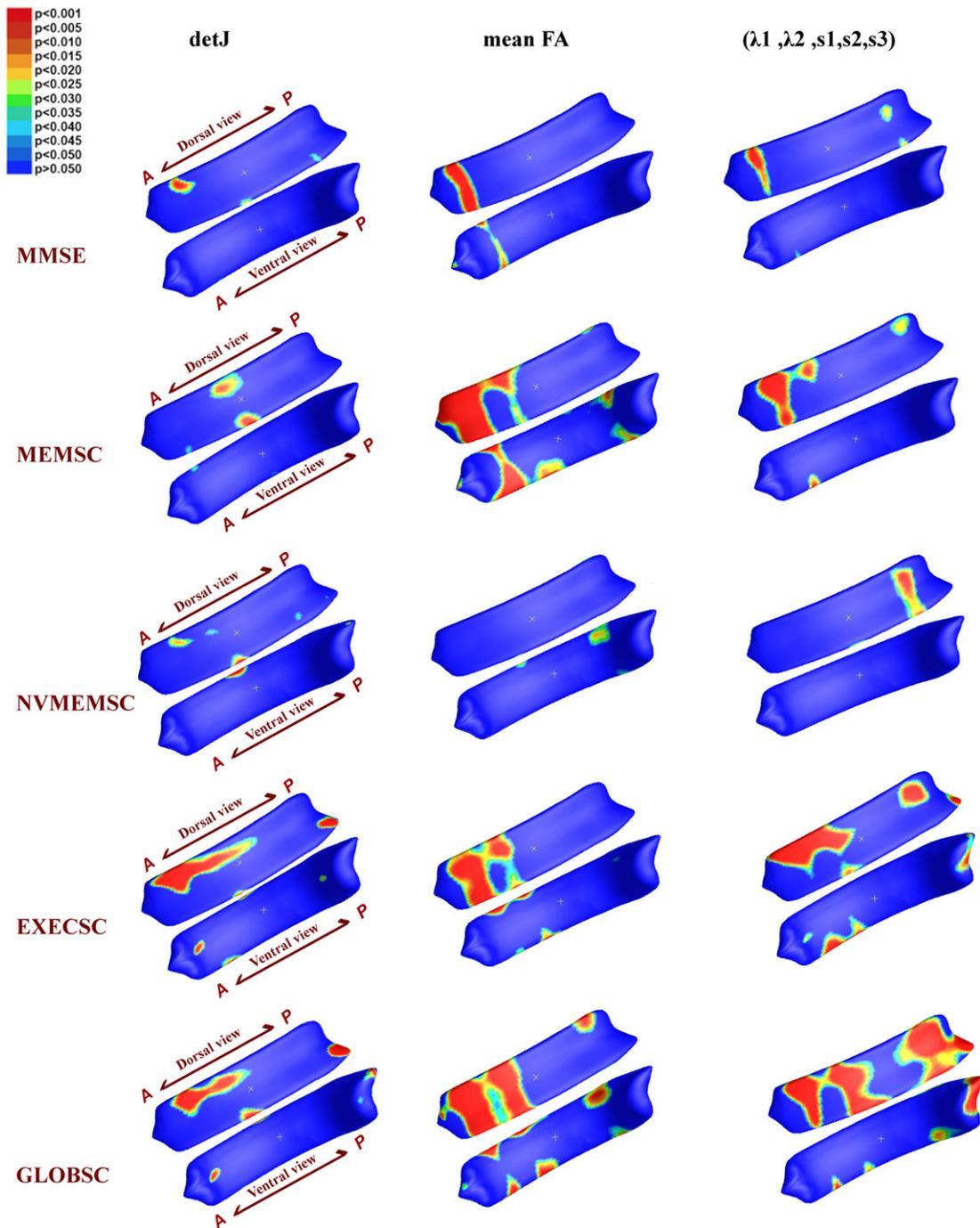
Fig. 4. Vertex-wise significance results of correlation analyses between detJ as well as mean FA vs. 5 neuropsychlogical scores. P- maps are smoothed using heat kernel algorithm (Chung et al., 2005).

DTI fusion analysis presented in this study yield higher statistical detection power, and may provide a new direction in analyzing subcortical WM structures.

4.0.1. Significance of the study

In the past decades, MCI has drawn increasing attention as a way to study the early evolution of AD, and as a potential target for early interventions. However, not all MCI patients will convert to AD as it is not a homogenous state and may also precede other types of dementia, such as vascular dementia (VaD). One of the main difficulties in accurately predicting the MCI - AD conversion is due to the co-morbidity and shared etiology with other types of disease (Meyer et al., 2002; Ott et al., 1995). In particular, CVD – precursors of VaD – are also important risk factors of AD (Newman et al., 2005; Vermeer et al., 2003). Epidemiological studies have shown that cardiovascular risk factors such as hypertension, high cholesterol, and diabetes are highly associated with cognitive decline and AD (de Bruijn and Ikram, 2014; Newman et al., 2005; Stampfer, 2006). Nevertheless, no established mechanisms clarify how CVD participates in the development of AD, and whether there is a dissociable impact of CVD and cardiovascular risk factors (CRF).
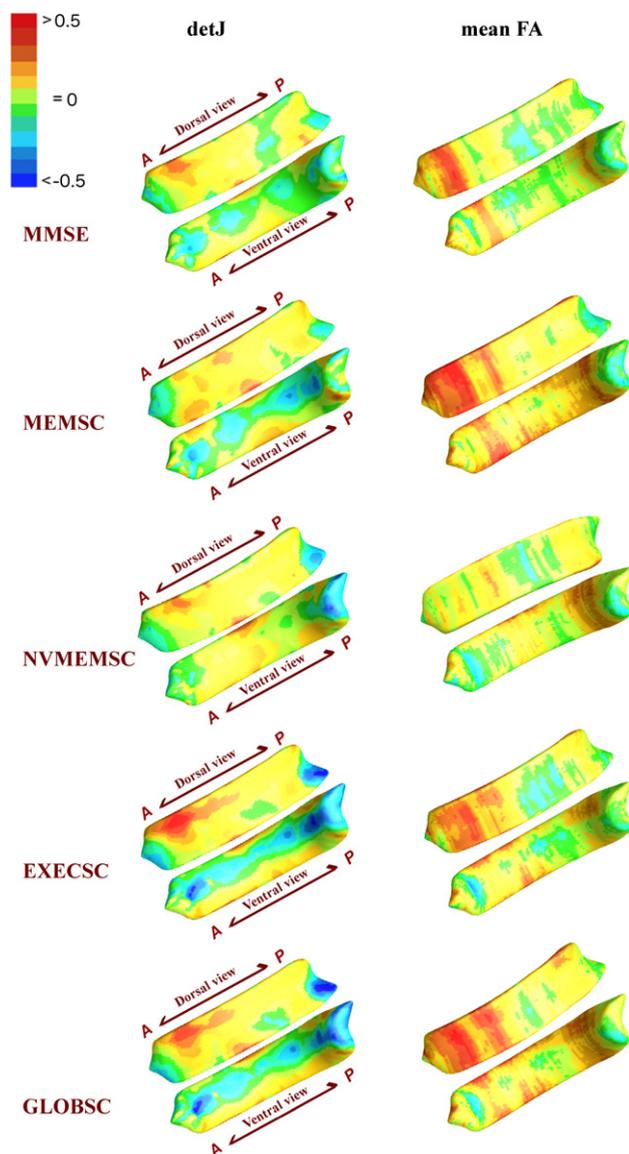
Fig. 5. Vertex-wise correlation coefficient maps have been generated based on det*J* (left column) and mean FA (right column), respectively. Compared this figure with Fig. 4, we can see the direction of the correlation analyses: nearly all the significant regions represent positive correlations.

from AD observed a slightly severe, but non-significant executive dysfunction than memory failure in autopsy-defined cerebrovascular disease group (Reed et al., 2007). Moreover, a study comparing cognitive profiles in MCI subjects with different etiologies reported no differences of memory or executive function between the vascular and non-vascular types of MCI (Loewenstein et al., 2006). These inconsistencies hint at the limitation of using neuropsychological patterns only as dissociable features for vascular injury/dementia (Reed et al., 2007).

With the advent of MRI, multiple modalities such as arterial spin labeling (ASL), structural and diffusion MRI have been utilized to investigate the vascular pathology on brain anatomy. It is widely accepted that vascular disease or risk factors are associated with an accelerated rate of cerebral atrophy (Barnes et al., 2013; Jochemsen et al., 2013; Kloppenborg et al., 2012) and decreased glucose metabolism (Chételat et al., 2013), while the information as to whether these associations are independent of MCI is minimal. In the handful of studies investigating vascular pathology in the context of MCI or AD, mixed results were reported. Specifically, a volume based T1-weighted MRI study on CC in AD, VaD as well as mild ambiguous subjects reported significantly smaller anterior and posterior CC regions in the AD group, significantly smaller anterior CC regions in the VaD group, and no difference in sub-clinical dementia group as compared to controls, while no differences between VaD and AD groups were detected (Hallam et al., 2008). A region of interest based DTI study on MCI subjects reported decreased WM integrity in selected frontal, temporal, parietal lobe regions as well as the corpus callosum in both groups of patients with and without subcortical vascular changes, while the WM alterations in the centrum semiovale and parietal lobe were believed to be more associated with the vascular pathology (Shim et al., 2008). A T1-MRI based study on cortical thickness and grey matter (GM) volume in MCI subjects with different levels of cardiovascular file profile observed an association between elevated vascular risk factors and atrophy in the temporal and parietal lobe - the same regions affected by AD (Cardenas et al., 2012).

Difficulties inherent in diagnosing and AD and VaD, and different inclusion criteria of vascular diseases clouded the interpretation of these studies. Moreover, limited statistical power of volume based methodologies and measurements focusing on single modality measurement further reduced the sensitivity of these studies to the potential neuroanatomical alterations lurking in pre-clinical stages. Therefore, in-vivo measurements with higher sensitivity are highly desired to further explore the concurrent but possibly distinct effects of CVD and MCI on the brain. In this work, we focused on neurodegenerative patterns in pre-dementia stages, and excluded compounding conditions such as stroke that directly alter brain anatomy. In the present study, the joint T1 and DTI measurement in 3D CC had successfully pinpointed dorsal anterior CC regions that significantly differed between MCI-l and MCI-h group of subjects. These findings provided new anatomical evidence for the distinctive impact of vascular pathology before clinical magnification of dementia, thus of great importance in early preventive intervention and in guiding therapeutical design. The sensitivity of our methodology and the relevance of detected anatomic alterations and the corresponding neuroanatomic and functional implications will be described in details in the next sections.

4.1. Methodological considerations

Postmortem and probabilistic tractography studies have shown that the CC is not a homogenous structure, in terms of fiber composition (Aboitiz et al., 1992) and topographical distribution (Park et al., 2008). Group differences of brain WM, including the CC, are typically analyzed based on whole structure volume or

A considerable number of researchers suggested a selective cognitive decline pattern associated with vascular pathology, and efforts have been made to differentiate vascular disease from AD or MCI using cognitive performance. Ingles et al. investigated the neuropsychological performance in elderly subjects 5 years before diagnosis, and reported a selectively low abstract reasoning performance in subjects who evolved toward vascular cognitive impairment compared to those who converted to AD or remained normal (Ingles et al., 2007). Marra et al. reported executive functioning problems in the vascular form of MCI subjects, whereas the degenerative form of MCI were mainly impaired in episodic memory tasks (Marra et al., 2011). Similar to these, greater impairments in executive function have been reported in MCI with a vascular component (Graham et al., 2004; Hayden et al., 2005; Nordlund et al., 2007; Nyström et al., 2015). However, there is no consensus on the executive dysfunction predominance of vascular pathology. A neurophysiological study aiming to discriminate cerebrovascular disease

some anatomically motivated partitions, voxels, midlines, or midplanes. The whole volume based method facilitates an intuitive and coarse estimation of CC anatomy (Ardekani et al., 2014; Zhu et al., 2013), but has been ineffective in detecting subtle anatomical changes. Studies based on subdivisions of the CC are more tuned to the heterogeneity of CC, but may easily be biased due to inconsistent classification (i.e. partitioning into 3, 5 or 7 compartments), as well as arbitrary delineation of subdivisions (Bachman et al., 2014; Frederiksen et al., 2011; Rosas et al., 2010). Voxel-based methods give poor localization of differences in anatomical regions compared to surface-based ones and may be contaminated by differently oriented tracts (O'Donnell et al., 2009), while midline- or midplane-based methods rely on assumptions that WM perpendicular to the mid-line or the mid-plane is uniformly distributed. The method introduced in this paper uses clearly defined CC regions traced in T1 images, that are largely preserved within tract information projected onto the surface of the corpus callosa. The 3D representations may better localize injury in heterogeneous CC, and may have higher statistical detection power to identify the neuro-circuit alterations underlying the observed anatomical alterations.

The vulnerability of the CC in MCI has been reported in both structural and diffusion studies (Di Paola et al., 2010; Hu et al., 2014; Teipel et al., 2011; Ukmar et al., 2008; Zhang et al., 2013, 2007; Zhuang et al., 2010). Structural MRI is a typical choice and has been effective in deciphering brain parenchyma loss (Serra et al., 2010; Teipel et al., 2002; Zhu et al., 2012), while DTI has been promising in characterizing white matter microstructure alterations (Karas et al., 2008; Teipel et al., 2011;Ukmar et al., 2008;Zhang et al., 2013, 2007;Zhuang et al., 2010). These previous studies have been analyzing the brain parenchyma or its diffusion properties on their own (Ukmar et al., 2008; Zhang et al., 2013, 2007), or by comparing them side-by-side (Di Paola et al., 2010; Rosas et al., 2010; Teipel et al., 2011). To the best of our knowledge, none have tried to truly combine these two features into one statistical analysis.

As shown in our study, measurements in both structural and diffusion aspects have given significant between group differences, confirming the concomitantly occurred parenchyma and diffuse injuries in CC. Group analyses based on structural information (det$J$ and ($s1, s2, s3$)) have successfully detected alterations in the mid-body to the posterior end, while group analyses based on diffusion information (mean FA and (λ_1, λ_2)) are more sensitive to alterations in the anterior and the posterior ends of CC. Here, for the first time, we fuse the T1-based morphometry information and DTI-based diffusion information into one, single analysis. In all three group-wise analyses, the fused method successfully outperforms analyses based on structural information or diffusion information alone. Moreover, in group comparisons between MCI-h and MCI-l group, only the fusion method reached overall significance, while no significance is detected if T1 and DTI measures are considered separately. These results show the feasibility of using the T1 and DTI fusion method to increase detection power.

4.2. Anatomic and functional implications

The corpus callosum spans the midline of the brain and possesses numerous connections to surrounding structures. At its most anterior end, the genu, WM tracts innervate the frontal lobes, and infarction of the genu has been reported to result in frontal lobe dysfunction (Buklina, 2005; Krupa and Bekiesinska-Figatowska, 2013; Miller and Cummings, 2007). The splenium, at the posterior end, lies in close proximity to the hippocampus through the amygdala (Kretschmann et al., 1998), and alterations of the splenium are often associated with impairments in memory and visual perception (Knyazeva, 2013; Rudge and Warrington, 1991). In our cohort of subjects, these anatomic-functional relationships have been further

validated in the correlation analysis of regional CC FA values with 5 neuropsychological tests. As shown in Fig. 4 and Fig. 5, executive functioning, verbal memory, and global cognitive profile, which are higher brain functions that are extensively involved frontal networks (Cummings, 1993; Hoffmann, 2013), showed significant associations with dorsal anterior CC, while nonverbal memory, which is highly correlated with hippocampus functioning (Bonner-Jackson et al., 2015), selectively correlates with the ventral posterior CC.

Thus, the anatomy of the dorsal anterior CC is more predictive of frontal lobe involved executive and verbal memory functions, while the posterior CC is more associated with temporal and parietal nonverbal memory. Taken together, the constellation of group-wise analysis and anatomical-neurophysiological correlations imply a main effect of MCI on medial to posterior cortex involved memory functions, while CVD and its risk factors add to the symptoms through frontal connections.

Comparing to controls, CCs in the MCI-h group presented similar but more extensive alterations than those from the MCI-l group, suggesting an 'interactive' impact of the vascular and neurodegenerative factors on brain morphometry. These are generally in line with anatomical findings showing associations between vascular brain injuries or risk factors and aggregated brain atrophy, especially in the parietal and temporal lobe (Cardenas et al., 2012; Villeneuve et al., 2014). In terms of the comparison within MCI subgroups, significant differences resided in the dorsal anterior CC, implying an 'additive' effect of vascular pathology on the brain frontal network that is differentiable from the non-vascular neurodegeneration influences. The frontal lobe hypo-perfusion detected by ASL-MRI has been reported to be associated with worse executive and memory function (Alosco et al., 2013). Vascular risk factors measured by FCRP and high-density lipoprotein cholesterol are found to link with thinner frontotemporal cortex (Villeneuve et al., 2014). In our study, the distinctive impact of the cardiovascular factor in the genu of CC is consistent with the anatomic relationship between cognitive profile and the frontal lobe (Villeneuve et al., 2014), and provides further neuroanatomic evidence supporting the neuropsychological findings of the selective executive dysfunction of vascular pathology (Hayden et al., 2005; Marra et al., 2011; Nordlund et al., 2007).

However, our implications for a vascular associated frontal lobe dominated cognitive functions needs to be interpreted with caution. As detected by the T1 and DTI joint analysis, broader areas including anterior, mid-body, and posterior CC showed different levels of alterations in the MCI-h group, while only the anterior regions reached group-wise significance. Hence, the significant alterations detected in genu between MCI with high and low vascular types does not mean that the anterior CC is the only region involved in vascular pathology. For instance, the conclusion in Villeneuve et al. (2014) is that vascular risk factors 'interact' with neurodegeneration factors in temporal and posterior lobe, and cause additional adverse effect on the frontal lobe. Further, reduced executive or global cognitive functioning implied by more severely altered genu does not necessarily lead to the assertion that cardiovascular factors impair executive functioning more severely than nonverbal memory. Previously, to validate the executive predominance model of vascular pathology, (Reed et al., 2007) hypothesized a lower executive performance than episodic memory performance in cases with autopsy-defined cerebrovascular diseases, but failed to detect a statistical significant differences between the two tests. Our study provides a potential interpretation to previous results that vascular pathology may accelerate the deterioration of multiple cognitive domains, with its influence on the frontal involved network especially dissociable from non-vascular neurodegeneration factors.

Our current study extend the database of vascular pathology on the brain in pre-dementia stages, and suggests an 'additive', albeit not 'dominant' effect of vascular associated impact on the frontal lobe, which may eventually lead to the refinement of the widely

accepted frontal predominancy theory. Our findings provide new neuroanatomical substrate of vascular contributions to cognitive impairment before the magnification of dementia, which may serve as a new biomarker that helps clinical diagnostic and therapeutical design.

5. Limitations and future directions

There are also several limitations of the presented study. First, due to the limited size of our cohort, we merged subjects with high FCRP and subjects with histories of myocardial infarction into one single group - the MCI-h group. We hope to enroll more subjects in the future, and refine our vascular model. Second, due to the large age range within our cohort, we used linear regression to factor out the effect of age. The effect of age on brain anatomy in elderly subjects has been widely accepted, and we did observe a significant linear relationship between age the surface diffusion indices as shown in Fig. 4. However, the use of linear regression does not rule out the possible existence of nonlinear relationship between age and brain anatomy. Third, here we only included the most representative univariate or multivariate measurements in our statistical analyses. Nonetheless, our methods can also be applied to other shape or diffusion measurements like thickness, mean diffusivity (MD), radial diffusivity (RD), and alike, as well as combinations among these. Fourth, it would be desirable to include other factors, like gender, gene, education and ethnicity in future analyses to derive a more comprehensive model.

In the future, we would also like to extend this method to to subdivide the CC into functionally or anatomically relevant regions, to further strengthen the interpretation of our results. For example, we could use a probabilistic tractography to the cortex or functional-based partition on the CC subregions (Park et al., 2008), especially where showed significant group differences, to investigate the association between regional CC alterations with disturbances in specific cortical domains. In addition, it would be important to track the mental status of patients, to see whether any of them transform into clinically diagnosed dementia. This may provide additional insight into the contribution of the vascular component in the conversion to Alzheimer's disease or other types of dementia.

Acknowledgments

References

Aboitiz, F., Scheibel, A.B., Fisher, R.S., Zaidel, E., 1992. Fiber composition of the human corpus callosum. Brain Res. 598 (1), 143–153.
Alosco, M.L., Gunstad, J., Jerskey, B.A., Xu, X., Clark, U.S., Hassenstab, J., Cote, D.M., Walsh, E.G., Labbe, D.R., Hoge, R., et al. 2013. The adverse effects of reduced cerebral perfusion on cognition and brain structure in older adults with cardio-vascular disease. Brain Behav. 3 (6), 626–636.
Ardekani, B.A., Bachman, A.H., Figarsky, K., Sidtis, J.J., 2014. Corpus callosum shape changes in early Alzheimer's disease: an MRI study using the oasis brain database. Brain Struct. Funct. 219 (1), 343–352.
Arsigny, V., Commowick, O., Pennec, X., Ayache, N., 2006. A log-Euclidean framework for statistics on diffeomorphisms. Medical Image Computing and Computer-Assisted Intervention-MICCAI 2006. Springer., pp. 924–931.
Bachman, A.H., Lee, S.H., Sidtis, J.J., Ardekani, B.A., 2014. Corpus callosum shape and size changes in early Alzheimer's disease: a longitudinal MRI study using the oasis brain database. J. Alzheimers Dis. 39 (1), 71–78.
Barnes, J., Carmichael, O.T., Leung, K.K., Schwarz, C., Ridgway, G.R., Bartlett, J.W., Malone, I.B., Schott, J.M., Rossor, M.N., Biessels, G.J., et al. 2013. Vascular and Alzheimer's disease markers independently predict brain atrophy rate in Alzheimer's disease neuroimaging initiative controls. Neurobiol. Aging 34 (8), 1996–2002.
Benjamini, Y., Hochberg, Y., 1995. Controlling the false discovery rate: a practical and powerful approach to multiple testing. J. R. Stat. Soc. Ser. B 289–300.

Bonner-Jackson, A., Mahmoud, S., Miller, J., Banks, S.J., 2015. Verbal and non-verbal memory and hippocampal volumes in a memory clinic population. Alzheimers Res. Ther. 7 (1), 1–10.
Buklina, S.B., 2005. The corpus callosum, interhemisphere interactions, and the function of the right hemisphere of the brain. Neurosci. Behav. Physiol. 35 (5), 473–480.
Cardenas, V.A., Reed, B., Chao, L.L., Chui, H., Sanossian, N., DeCarli, C.C., Mack, W., Kramer, J., Hodis, H.N., Yan, M., et al. 2012. Associations among vascular risk factors, carotid atherosclerosis, and cortical volume and thickness in older adults. Stroke 43 (11), 2865–2870.
Chételat, G., Landeau, B., Salmon, E., Yakushev, I., Bahri, M.A., Mézenge, F., Perrotin, A., Bastin, C., Manrique, A., Scheurich, A., et al. 2013. Relationships between brain metabolism decrease in normal aging and changes in structural and functional connectivity. Neuroimage 76, 167–177.
Chui, H.C., 2006. Vascular cognitive impairment: today and tomorrow. Alzheimers Dement. 2 (3), 185–194.
Chung, M.K., Robbins, S.M., Dalton, K.M., Davidson, R.J., Alexander, A.L., Evans, A.C., 2005. Cortical thickness analysis in autism with heat kernel smoothing. NeuroImage 25 (4), 1256–1265.
Cummings, J.L., 1993. Frontal-subcortical circuits and human behavior. Arch. Neurol. 50 (8), 873.
de Bruijn, R.F.A.G., Ikram, M.A., 2014. Cardiovascular risk factors and future risk of Alzheimer's disease. BMC Med. 12 (1), 130.
Delano-Wood, L., Bondi, M.W., Jak, A.J., Horne, N.R., Schweinsburg, B.C., Frank, L.R., Wierenga, C.E., Delis, D.C., Theilmann, R.J., Salmon, D.P., 2010. Stroke risk modifies regional white matter differences in mild cognitive impairment. Neurobiol. Aging 31 (10), 1721–1731.
Di Paola, M., Di Iulio, F., Cherubini, A., Blundo, C., Casini, A.R., Sancesario, G., Passafiume, D., Caltagirone, C., Spalletta, G., 2010. When, where, and how the corpus callosum changes in MCI and ad a multimodal MRI study. Neurology 74 (14), 1136–1142.
Dimitra, S., Verganelakis, D.A., Gotsis, E., Toulas, P., Papatriantafillou, J., Karageorgiou, C., Thomaides, T., Kapsalaki, E.Z., Hadjigeorgiou, G., Papadimitriou, A., 2013. Diffusion tensor imaging (DTI) in the detection of white matter lesions in patients with mild cognitive impairment (MCI). Acta Neurol. Belg. 113 (4), 441–451.
Frederiksen, K.S., Garde, E., Skimminge, A., Ryberg, C., Rostrup, E., Baaré, W.F.C., Siebner, H.R., Hejl, A.-M., Leffers, A.-M., Waldemar, G., 2011. Corpus callosum atrophy in patients with mild Alzheimer's disease. Neurodegener. Dis. 8 (6), 476–482.
Friedman, J.I., Tang, C.Y., de Haas, H.J., Changchien, L., Goliasch, G., Dabas, P., Wang, V., Fayad, Z.A., Fuster, V., Narula, J., 2014. Brain imaging changes associated with risk factors for cardiovascular and cerebrovascular disease in asymptomatic patients. J. Am. Coll. Cardiol. Img. 7 (10), 1039–1053.
Garcia-Alloza, M., Gregory, J., Kuchibhotla, K.V., Fine, S., Wei, Y., Ayata, C., Frosch, M.P., Greenberg, S.M., Bacskai, B.J., 2011. Cerebrovascular lesions induce transient β-amyloid deposition. Brain 134 (12), 3694–3704.
Gons, R.A.R., van Oudheusden, L.J.B., de Laat, K.F., van Norden, A.G.W., van Uden, I.W.M., Norris, D.G., Zwiers, M.P., van Dijk, E., de Leeuw, F.-E., 2012. Hypertension is related to the microstructure of the corpus callosum: the run DMC study. J. Alzheimers Dis. 32 (3), 623–631.
Gorelick, P.B., Scuteri, A., Black, S.E., DeCarli, C., Greenberg, S.M., Iadecola, C., Launer, L.J., Laurent, S., Lopez, O.L., Nyenhuis, D., et al. 2011. Vascular contributions to cognitive impairment and dementia a statement for healthcare professionals from the American Heart Association/American stroke association. Stroke 42 (9), 2672–2713.
Graham, N.L., Emery, T., Hodges, J.R., 2004. Distinctive cognitive profiles in Alzheimer's disease and subcortical vascular dementia. J. Neurol. Neurosurg. Psychiatry 75 (1), 61–71.
Hallam, B.J., Brown, W.S., Ross, C., Buckwalter, J.G., Bigler, E.D., Tschanz, J.T., Norton, M.C., Welsh-Bohmer, K.A., Breitner, J.C., 2008. Regional atrophy of the corpus callosum in dementia. J. Int. Neuropsychol. Soc. 14 (03), 414–423.
Hayden, K.M., Warren, L.H., Pieper, C.F., Østbye, T., Tschanz, J.T., Norton, M.C., Breitner, J.C.S., Welsh-Bohmer, K.A., 2005. Identification of vad and ad prodromes: the cache county study. Alzheimers Dement. 1 (1), 19–29.
Hoffmann, M., 2013. The human frontal lobes and frontal network systems: an evolutionary, clinical, and treatment perspective. ISRN Neurol. 2013,
Hu, Z., Wu, L., Jia, J., Han, Y., 2014. Advances in longitudinal studies of amnestic mild cognitive impairment and Alzheimer's disease based on multi-modal MRI techniques. Neurosci. Bull. 30 (2), 198–206.
Iadecola, C., 2013. The pathobiology of vascular dementia. Neuron 80 (4), 844–866.
Ingles, J.L., Boulton, D.C., Fisk, J.D., Rockwood, K., 2007. Preclinical vascular cognitive impairment and Alzheimer disease neuropsychological test performance 5 years before diagnosis. Stroke 38 (4), 1148–1153.
Jenkinson, M., Bannister, P., Brady, M., Smith, S., 2002. Improved optimization for the robust and accurate linear registration and motion correction of brain images. Neuroimage 17 (2), 825–841.
Jochemsen, H.M., Muller, M., Visseren, F.L., Scheltens, P., Vincken, K.L., Mali, W.P., van der Graaf, Y., Geerlings, M.I., 2013. Blood pressure and progression of brain atrophy: the smart-MR study. JAMA Neurol. 70 (8), 1046–1053.
Kalaria, R.N., Akinyemi, R., Ihara, M., 2012. Does vascular pathology contribute to Alzheimer changes? J. Neurol. Sci. 322 (1), 141–147.
Kantarci, K., Petersen, R.C., Boeve, B.F., Knopman, D.S., Weigand, S.D., OBrien, P.C., Shiung, M.M., Smith, G.E., Ivnik, R.J., Tangalos, E.G., et al. 2005. DWI predicts future progression to alzheimer disease in amnestic mild cognitive impairment. Neurology 64 (5), 902–904.
Karas, G., Sluimer, J., Goekoop, R., Van Der Flier, W., Rombouts, S., Vrenken, H., Scheltens, P., Fox, N., Barkhof, F., 2008. Amnestic mild cognitive impairment:

structural MR imaging findings predictive of conversion to Alzheimer disease. Am. J. Neuroradiol. 29 (5), 944–949.

Kloppenborg, R.P., Nederkoorn, P.J., Grool, A.M., Vincken, K.L., Mali, W.P.T.M., Vermeulen, M., van der Graaf, Y., Geerlings, M.I., 2012. Cerebral small-vessel disease and progression of brain atrophy the smart-MR study. Neurology 79 (20), 2029–2036.

Knyazeva, M.G., 2013. Splenium of corpus callosum: patterns of interhemispheric interaction in children and adults. Neural Plast. 2013,

Kretschmann, H.-J., Weinrich, W., Fiekert, W., 1998. Neurofunctional systems: 3D reconstructions with correlated neuroimaging. Univ of California Press.

Krupa, K., Bekiesinska-Figatowska, M., 2013. Congenital and acquired abnormalities of the corpus callosum: a pictorial essay. Biomed. Res. Int. 2013,

Lao, Y., Law, M., Shi, J., Gajawelli, N., Haas, L., Wang, Y., Leporé, N., 2015. A t1 and DTI fused 3D corpus callosum analysis in pre-vs. post-season contact sports players. Tenth International Symposium on Medical Information Processing and Analysis. 92870O.

Lao, Y., Wang, Y., Shi, J., Ceschin, R., Nelson, M.D., Panigrahy, A., Leporé, N., 2014. Thalamic alterations in preterm neonates and their relation to ventral striatum disturbances revealed by a combined shape and pose analysis. Brain Struct. Funct. 1–20.

Lepore, F., Brun, C., Chou, Y.-Y., Chiang, M.-C., Dutton, R.A., Hayashi, K.M., Luders, E., Lopez, O.L., Aizenstein, H.J., Toga, A.W., et al. 2008. Generalized tensor-based morphometry of HIV/AIDS using multivariate statistics on deformation tensors. IEEE Trans. Med. Imaging 27 (1), 129–141.

Loewenstein, D.A., Acevedo, A., Agron, J., Issacson, R., Strauman, S., Crocco, E., Barker, W.W., Duara, R., 2006. Cognitive profiles in Alzheimer's disease and in mild cognitive impairment of different etiologies. Dement. Geriatr. Cogn. Disord. 21 (5-6), 309–315.

Luchsinger, J.A., Tang, M.-X., Stern, Y., Shea, S., Mayeux, R., 2001. Diabetes mellitus and risk of Alzheimer's disease and dementia with stroke in a multiethnic cohort. Am. J. Epidemiol. 154 (7), 635–641.

Marra, C., Ferraccioli, M., Gabriella Vita, M., Quaranta, D., Gainotti, G., 2011. Patterns of cognitive decline and rates of conversion to dementia in patients with degenerative and vascular forms of mci. Curr. Alzheimer Res. 8 (1), 24–31.

Mather, M., Harley, C.W., 2016. The locus coeruleus: Essential for Maintaining Cognitive Function and the Aging Brain. Trends Cogn. Sci. 20 (3), 214–226.

Meyer, J.S., Xu, G., Thornby, J., Chowdhury, M.H., Quach, M., 2002. Is mild cognitive impairment prodromal for vascular dementia like Alzheimer's disease? Stroke 33 (8), 1981–1985.

Miller, B.L., Cummings, J.L., 2007. The Human Frontal Lobes: Functions and Disorders. Guilford Press.

Mungas, D., Reed, B.R., Kramer, J.H., 2003. Psychometrically matched measures of global cognition, memory, and executive function for assessment of cognitive decline in older persons. Neuropsychology 17 (3), 380.

Newman, A.B., Fitzpatrick, A.L., Lopez, O., Jackson, S., Lyketsos, C., Jagust, W., Ives, D., DeKosky, S.T., Kuller, L.H., 2005. Dementia and Alzheimer's disease incidence in relationship to cardiovascular disease in the cardiovascular health study cohort. J. Am. Geriatr. Soc. 53 (7), 1101–1107.

Nichols, T.E., Holmes, A.P., 2001. Nonparametric permutation tests for functional neuroimaging: a primer with examples. Hum. Brain Mapp. 15 (1), 1–25.

Nordlund, A., Rolstad, S., Klang, O., Lind, K., Hansen, S., Wallin, A., 2007. Cognitive profiles of mild cognitive impairment with and without vascular disease. Neuropsychology 21 (6), 706.

Nyström, O., Wallin, A., Nordlund, A., 2015. MCI of different etiologies differ on the cognitive assessment battery. Acta Neurol. Scand. 132 (1), 31–36.

O'Donnell, L.J., Westin, C.-F., Golby, A.J., 2009. Tract-based morphometry for white matter group analysis. Neuroimage 45 (3), 832–844.

Ott, A., Breteler, M., Van Harskamp, F., Claus, J.J., Van Der Cammen, T.J., Grobbee, D.E., Hofman, A., 1995. Prevalence of Alzheimer's disease and vascular dementia: association with education. The Rotterdam study. Bmj 310 (6985), 970–973.

Park, H.-J., Kim, J.J., Lee, S.-K., Seok, J.H., Chun, J., Kim, D.I., Lee, J.D., 2008. Corpus callosal connection mapping using cortical gray matter parcellation and DT-MRI. Hum. Brain Mapp. 29 (5), 503–516.

Posner, H.B., Tang, M.-X., Luchsinger, J., Lantigua, R., Stern, Y., Mayeux, R., 2000. The relationship of hypertension in the elderly to ad, vascular dementia, and cognitive function. Neurology 58 (8), 1175–1181.

Rajagopalan, V., Scott, J., Habas, P.A., Kim, K., Rousseau, F., Glenn, O.A., Barkovich, A.J., Studholme, C., 2012. Mapping directionality specific volume changes using tensor based morphometry: an application to the study of gyrogenesis and lateralization of the human fetal brain. Neuroimage 63 (2), 947–958.

Reed, B.R., Mungas, D.M., Kramer, J.H., Ellis, W., Vinters, H.V., Zarow, C., Jagust, W.J., Chui, H.C., 2007. Profiles of neuropsychological impairment in autopsy-defined Alzheimer's disease and cerebrovascular disease. Brain 130 (3), 731–739.

Rosas, H.D., Lee, S.Y., Bender, A.C., Zaleta, A.K., Vangel, M., Yu, P., Fischl, B., Pappu, V., Onorato, C., Cha, J.-H., et al. 2010. Altered white matter microstructure in the corpus callosum in Huntington's disease: implications for cortical disconnection. Neuroimage 49 (4), 2995–3004.

Rudge, P., Warrington, E.K., 1991. Selective impairment of memory and visual perception in splenial tumours. Brain 114 (1), 349–360.

Serra, L., Cercignani, M., Lenzi, D., Perri, R., Fadda, L., Caltagirone, C., Macaluso, E., Bozzali, M., 2010. Grey and white matter changes at different stages of Alzheimer's disease. J. Alzheimers Dis. 19 (1), 147–159.

Shim, Y.S., Yoon, B., Shon, Y.-M., Ahn, K.-J., Yang, D.-W., 2008. Difference of the hippocampal and white matter microalterations in MCI patients according to the severity of subcortical vascular changes: neuropsychological correlates of diffusion tensor imaging. Clin. Neurol. Neurosurg. 110 (6), 552–561.

Stampfer, M.J., 2006. Cardiovascular disease and Alzheimer's disease: common links. J. Intern. Med. 260 (3), 211–223.

Székely, G.J., Rizzo, M.L., et al. 2009. Brownian distance covariance. Ann. Appl. Stat. 3 (4), 1236–1265.

Teipel, S.J., Bayer, W., Alexander, G.E., Teichberg, D., Kulic, L., Schapiro, M.B., Möller, H.-J., Rapoport, S.I., Hampel, H., 2002. Progression of corpus callosum atrophy in Alzheimer disease. Arch. Neurol. 59 (2), 243–248.

Teipel, S.J., Meindl, T., Grinberg, L., Grothe, M., Cantero, J.L., Reiser, M.F., Möller, H.-J., Heinsen, H., Hampel, H., 2011. The cholinergic system in mild cognitive impairment and Alzheimer's disease: an in vivo MRI and DTI study. Hum. Brain Mapp. 32 (9), 1349–1362.

P., F., Toussaint, N., Souplet, J., 2007. Medinria: Medical image navigation and research tool by INRIA. Proc. of MICCAI'07 Workshop on Interaction in medical image analysis and visualization

Ukmar, M., Makuc, E., Onor, M.L., Garbin, G., Trevisiol, M., Cova, M.A., 2008. Evaluation of white matter damage in patients with Alzheimer's disease and in patients with mild cognitive impairment by using diffusion tensor imaging. Radiol. Med. 113 (6), 915–922.

Vermeer, S.E., Prins, N.D., den Heijer, T., Hofman, A., Koudstaal, P.J., Breteler, M.M., 2003. Silent brain infarcts and the risk of dementia and cognitive decline. N. Engl. J. Med. 348 (13), 1215–1222.

Villeneuve, S., Reed, B.R., Madison, C.M., Wirth, M., Marchant, N.L., Kriger, S., Mack, W.J., Sanossian, N., DeCarli, C., Chui, H.C., et al. 2014. Vascular risk and aβ interact to reduce cortical thickness in ad vulnerable brain regions. Neurology 83 (1), 40–47.

Wang, Y., Chan, T.F., Toga, A.W., Thompson, P.M., 2009. Multivariate tensor-based brain anatomical surface morphometry via holomorphic one-forms. International Conference on Medical Image Computing and Computer-Assisted Intervention. pp. 337–344.

Wang, Y., Song, Y., Rajagopalan, P., An, T., Liu, K., Chou, Y.-Y., Gutman, B., Toga, A.W., Thompson, P.M., 2011a. Surface-based TBM boosts power to detect disease effects on the brain: An n= 804 ADNI study. Neuroimage 56 (4), 1993–2010.

Wang, Y., Song, Y., Rajagopalan, P., An, T., Liu, K., Chou, Y.-Y., Gutman, B., Toga, A.W., Thompson, P.M., 2011b. Surface-based TBM boosts power to detect disease effects on the brain: An N= 804 ADNI study. Neuroimage 56 (4), 1993–2010.

Zhang, Y., Schuff, N., Camacho, M., Chao, L.L., Fletcher, T.P., Yaffe, K., Woolley, S.C., Madison, C., Rosen, H.J., Miller, B.L., et al. 2013. MRI markers for mild cognitive impairment: comparisons between white matter integrity and gray matter volume measurements. PloS one 8 (6), e66367.

Zhang, Y., Schuff, N., Jahng, G.-H., Bayne, W., Mori, S., Schad, L., Mueller, S., Du, A.-T., Kramer, J., Yaffe, K., et al. 2007. Diffusion tensor imaging of cingulum fibers in mild cognitive impairment and Alzheimer disease. Neurology 68 (1), 13–19.

Zhu, M., Gao, W., Wang, X., Shi, C., Lin, Z., 2012. Progression of corpus callosum atrophy in early stage of Alzheimers disease: MRI based study. Acad. Radiol. 19 (5), 512–517.

Zhu, M., Wang, X., Gao, W., Shi, C., Ge, H., Shen, H., Lin, Z., 2013. Corpus callosum atrophy and cognitive decline in early Alzheimer's disease: longitudinal MRI study. Dement. Geriatr. Cogn. Disord. 37 (3-4), 214–222.

Zhuang, L., Wen, W., Zhu, W., Trollor, J., Kochan, N., Crawford, J., Reppermund, S., Brodaty, H., Sachdev, P., 2010. White matter integrity in mild cognitive impairment: a tract-based spatial statistics study. Neuroimage 53 (1), 16–25.